AFRL-AFOSR-VA-TR-2016-0229

Coherent Structures in Plasmas Relevant to Electric Propulsion

Mark Cappelli
LELAND STANFORD JUNIOR UNIV CA

06/24/2016
Final Report

Air Force Research Laboratory
AF Office Of Scientific Research (AFOSR)/ RTA1
Arlington, Virginia 22203
Air Force Materiel Command

REPORT DOCUMENTATION PAGE

Form Approved
OMB No. 0704-0188

PLEASE DO NOT RETURN YOUR FORM TO THE ABOVE ORGANIZATION.

1. REPORT DATE *(DD-MM-YYYY)*	2. REPORT TYPE	3. DATES COVERED *(From - To)*
09-06-2016	Final Performance Report	May 2014 - Jun 2016

4. TITLE AND SUBTITLE

Coherent Structures in Plasmas Relevant to Electric Propulsion

5a. CONTRACT NUMBER
N/A

5b. GRANT NUMBER
FA9550-14-1-0017

5c. PROGRAM ELEMENT NUMBER

6. AUTHOR(S)

Mark Cappelli (PI: Stanford)
Yevgeny Raitses (PI: Princeton)
Igor Kagonavich (PI: Princeton)

5d. PROJECT NUMBER

5e. TASK NUMBER

5f. WORK UNIT NUMBER

7. PERFORMING ORGANIZATION NAME(S) AND ADDRESS(ES)

Board of Trustees of the Leland Stanford Junior University
3160 Porter Drive, Ste 100
Palo Alto, CA 94304-8445

8. PERFORMING ORGANIZATION REPORT NUMBER

9. SPONSORING/MONITORING AGENCY NAME(S) AND ADDRESS(ES)

USAF, AFRL DUNS 143574726
AF Office of Scientific Research
875 North Randolph Street, Rm 3112
Arlington, VA 22203-1954
Paula Poppy 703-588-1929 paula.poppy@us.af.mil

10. SPONSOR/MONITOR'S ACRONYM(S)

11. SPONSOR/MONITOR'S REPORT NUMBER(S)

12. DISTRIBUTION/AVAILABILITY STATEMENT

A

13. SUPPLEMENTARY NOTES

N/A

14. ABSTRACT

Magnetized plasmas in E x B configurations exhibit complex behavior resulting in variety of turbulent and coherent fluctuations that can critically affect E x B plasma thruster devices and performance. Rotating structures have been observed in laboratory and technological plasma devices with magnetized electrons and non-magnetized ions. These oscillations have low mode number with a characteristic frequency that lies between the electron and ion gyro-frequencies. Experimental studies of Hall and Penning discharges demonstrated that low frequency (10's kHz) disturbances contribute to electron cross-field transport. Studies carried out in mesoscale magnetrons place these coherent fluctuations at much higher frequencies (100's of kHz) and also contribute substantially to the electron transport. For Hall thrusters, electron cross-field transport is of practical importance because it diminishes the thrust efficiency. Fluctuation-induced transport reduces the local electric field, potentially leading to increased plume divergence and thruster wall erosion. This program is to better understand the physics behind these fluctuations and their relevance to propulsion devices through experimental, theoretical, and numerical studies.

15. SUBJECT TERMS

Plasma instabilities in magnetized discharges, plasma diagnostics, theoretical plasma physics, plasma kinetic simulations.

16. SECURITY CLASSIFICATION OF:			17. LIMITATION OF ABSTRACT	18. NUMBER OF PAGES	19a. NAME OF RESPONSIBLE PERSON
a. REPORT	b. ABSTRACT	c. THIS PAGE			Mark A. Cappelli (PI)
U	U	U	SAR	15	19b. TELEPHONE NUMBER *(Include area code)* 650-725-1745

Reset

INSTRUCTIONS FOR COMPLETING SF 298

1. REPORT DATE. Full publication date, including day, month, if available. Must cite at least the year and be Year 2000 compliant, e.g. 30-06-1998; xx-06-1998; xx-xx-1998.

2. REPORT TYPE. State the type of report, such as final, technical, interim, memorandum, master's thesis, progress, quarterly, research, special, group study, etc.

3. DATES COVERED. Indicate the time during which the work was performed and the report was written, e.g., Jun 1997 - Jun 1998; 1-10 Jun 1996; May - Nov 1998; Nov 1998.

4. TITLE. Enter title and subtitle with volume number and part number, if applicable. On classified documents, enter the title classification in parentheses.

5a. CONTRACT NUMBER. Enter all contract numbers as they appear in the report, e.g. F33615-86-C-5169.

5b. GRANT NUMBER. Enter all grant numbers as they appear in the report, e.g. AFOSR-82-1234.

5c. PROGRAM ELEMENT NUMBER. Enter all program element numbers as they appear in the report, e.g. 61101A.

5d. PROJECT NUMBER. Enter all project numbers as they appear in the report, e.g. 1F665702D1257; ILIR.

5e. TASK NUMBER. Enter all task numbers as they appear in the report, e.g. 05; RF0330201; T4112.

5f. WORK UNIT NUMBER. Enter all work unit numbers as they appear in the report, e.g. 001; AFAPL30480105.

6. AUTHOR(S). Enter name(s) of person(s) responsible for writing the report, performing the research, or credited with the content of the report. The form of entry is the last name, first name, middle initial, and additional qualifiers separated by commas, e.g. Smith, Richard, J, Jr.

7. PERFORMING ORGANIZATION NAME(S) AND ADDRESS(ES). Self-explanatory.

8. PERFORMING ORGANIZATION REPORT NUMBER. Enter all unique alphanumeric report numbers assigned by the performing organization, e.g. BRL-1234; AFWL-TR-85-4017-Vol-21-PT-2.

9. SPONSORING/MONITORING AGENCY NAME(S) AND ADDRESS(ES). Enter the name and address of the organization(s) financially responsible for and monitoring the work.

10. SPONSOR/MONITOR'S ACRONYM(S). Enter, if available, e.g. BRL, ARDEC, NADC.

11. SPONSOR/MONITOR'S REPORT NUMBER(S). Enter report number as assigned by the sponsoring/ monitoring agency, if available, e.g. BRL-TR-829; -215.

12. DISTRIBUTION/AVAILABILITY STATEMENT. Use agency-mandated availability statements to indicate the public availability or distribution limitations of the report. If additional limitations/ restrictions or special markings are indicated, follow agency authorization procedures, e.g. RD/FRD, PROPIN, ITAR, etc. Include copyright information.

13. SUPPLEMENTARY NOTES. Enter information not included elsewhere such as: prepared in cooperation with; translation of; report supersedes; old edition number, etc.

14. ABSTRACT. A brief (approximately 200 words) factual summary of the most significant information.

15. SUBJECT TERMS. Key words or phrases identifying major concepts in the report.

16. SECURITY CLASSIFICATION. Enter security classification in accordance with security classification regulations, e.g. U, C, S, etc. If this form contains classified information, stamp classification level on the top and bottom of this page.

17. LIMITATION OF ABSTRACT. This block must be completed to assign a distribution limitation to the abstract. Enter UU (Unclassified Unlimited) or SAR (Same as Report). An entry in this block is necessary if the abstract is to be limited.

Final Technical Report

Coherent Structures in Plasmas Relevant to Electric Propulsion

AFOSR Grant FA9550-14-1-0017

Mark Cappelli
Principal Investigator, *Stanford University, CA*
and

Yevgeny Raitses
Co-Principal Investigator, *Princeton University, Princeton, NJ*
Igor Kaganovich,
Co-Principal Investigator, *Princeton Plasma Physics Laboratory, Princeton, NJ*

Prepared for:
Dr. Mitat A. Birkan
AFOSR Program Manager

Introduction

Several modern space propulsion devices exploit the acceleration of propellant via the production of a magnetized plasma, some, in conditions where there are crossed electric and magnetic fields (e.g., Hall thrusters, Cusped Field Thrusters). These thrusters share several features that are in common with other magnetized cross-field plasma sources such as magnetron and Penning discharges. Magnetized plasmas in cross-field configurations exhibit complex nonlinear behavior resulting in variety of turbulent and coherent fluctuations that can critically affect thruster operation and performance. Rotating structures have been observed in a variety of laboratory and technological plasma devices with magnetized electrons and non-magnetized or weakly magnetized ions. These oscillations usually have low mode number with a characteristic frequency that lies between the electron and ion gyro-frequencies, i.e., $\Omega_{ce} << \omega \leq \Omega_{ci}$. Experimental studies of Hall thrusters and Penning discharges demonstrated that low frequency (10's kHz) spoke oscillations contribute to anomalous electron cross-field transport. Studies carried out in smaller devices, such as mesoscale magnetrons, place these coherent fluctuations at much higher frequencies (100's of kHz), and also contribute substantially to the electron transport. For Hall thrusters, electron cross-field transport is of practical importance because it diminishes the thrust efficiency. Fluctuation-induced transport reduces the local electric field, potentially leading to increased plume divergence and thruster wall erosion. This program is to better understand the physics behind these fluctuations and their relevance to propulsion devices. Our experiments are primarily carried out on Penning discharges (Princeton Plasma Physics Laboratory [PPPL] and Princeton University), and on magnetron discharges (Stanford), with some studies for comparisons to cylindrical Hall thrusters (PPPL and Princeton University) and cylindrical cusped field thrusters (Stanford), referred to here as CHT and CCFT for short. Both institutions have also been actively developing theory and simulations of the development of these coherent structures.

Research Background

Magnetized plasmas in cross-field discharge devices exhibit complex nonlinear behavior resulting in a variety of turbulent fluctuations and structures that critically affect operation and performance of these devices. E×B rotating structures sometimes referred to as rotating spoke oscillations have been observed in a variety of laboratory and technologically important plasma devices with magnetized electrons and non-magnetized or weakly magnetized ions. These devices include Hall thrusters, Penning discharges, and sputtering magnetrons. These oscillations usually have low mode number with a characteristic frequency of $\Omega_{ce} << \omega \leq \Omega_{ci}$, where Ω_{ce} and Ω_{ci} are the gyrofrequency of electrons and ions, respectively. Recent experimental studies of Hall thrusters and Penning discharges demonstrated that low frequency (1-10's of kHz) spoke oscillations are responsible for anomalous electron cross-field transport. In the magnetron thruster studies with segmented anodes (yet unpublished, see below), these instabilities, which appear to be gradient-drift driven in this device, are also responsible for the cross-field discharge current). For Hall thrusters, electron cross-field transport is of practical importance because it diminishes the thruster efficiency, which is the ratio of the plasma jet power to the input electric power. If the electric field decreases with increased cross-field transport, it can cause plume divergence and thruster wall erosion. Our recent measurements in Cylindrical Hall thrusters (CHT) (Fig. 1a) and Penning discharges (Fig. 1b) revealed a strong dependence of spoke oscillations on the input discharge parameters, including gas, gas pressure, the magnetic field, and the electron injection from the cathode[1, 2]. Similar observations have been reported for conventional state-of-the-art Hall thrusters.

The moving spoke is a plasma non-uniformity that rotates usually in the *E*×*B* direction. The spoke can appear in different modes, but for CHTs, Penning discharges and cylindrical magnetrons, the most common is the *m* =1 mode [1-3] (Fig. 2). In CHT and Penning discharges, the spoke was observed with a high-speed CCD camera and Langmuir probe measurements [3].

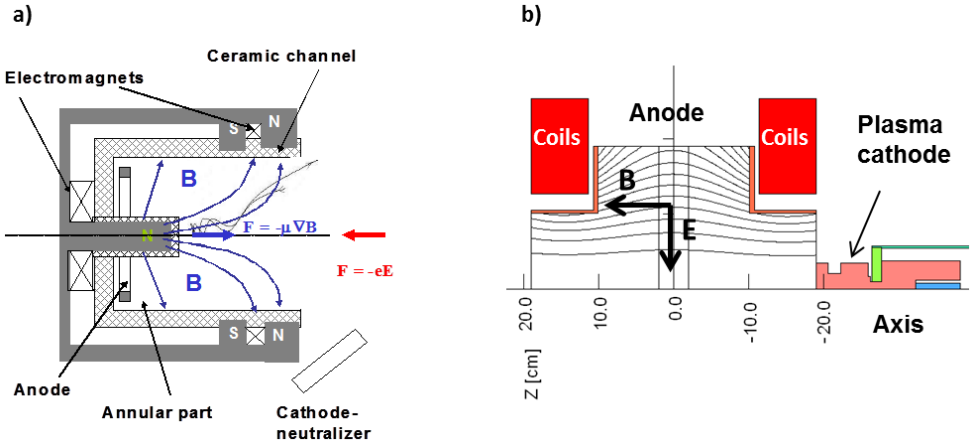

Figure 1. Schematics of E×B configurations of the cylindrical Hall thruster (a) and the Penning plasma discharge (b) [1, 2].

The spoke appeared on the camera as a spot of increased light emission that rotates in the azimuthal direction with the translation speed of an order of magnitude slower than the local E×B drift speed. Similar observations were also reported for the annular Hall thrusters [4] and other plasma devices. On probes immersed in CHT and Penning plasmas, the spoke manifests itself through azimuthal oscillations of plasma potential, electron temperature and plasma density.

Naturally, the spoke is a consequence of one or coupled multiple instabilities of the cross-field plasma discharge. Our recent studies on Penning discharges provided new insights on the

fundamental role of gradient drift (modified Simon-Hon type) instabilities driven by gradients of plasma density, temperature and magnetic field [5]. Ionization instabilities may be coupled to this electrostatic instability giving raise the formation of rotating plasma structures. We have identified in the experiment and simulations a strong connection between these plasma structures and electron transport. This connection is responsible for the mode transition, facility effects, and effects of the magnetic field, effects of device (e.g. thruster) geometry and materials on plasma structures.

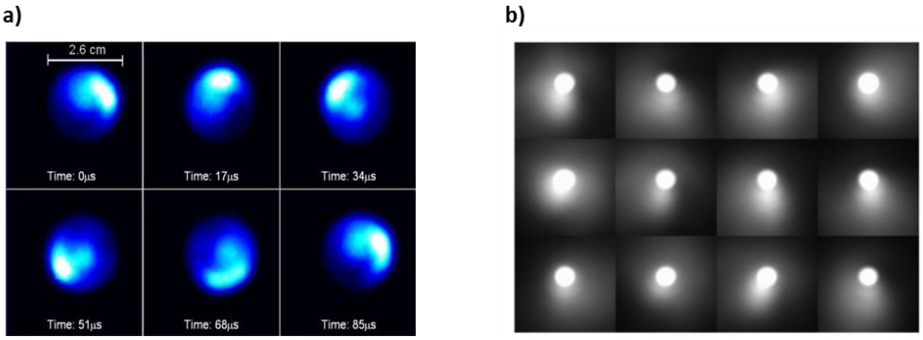

Figure 2. E×B rotating spoke in CHT thruster (a) and Penning discharge (b).

The overall physics which we have discerned from our integrated experimental, simulations and theoretical efforts (described below) is as follows: small-scale phenomena such as microturbulence is responsible for anomalous transport, which determines both the electric field and pressure gradients, which in turn, can induce large-scale gradient-driven instabilities forming plasma strictures such as spokes. The dynamics of the plasma structure is also determined by a relatively slow rotation of ions due to a partial magnetization or momentum conservation, and charge exchange collisions.

Understating of micro turbulence at the scale comparable to the electron gyro radius and its effects, including the formation of the plasma structures requires a kinetic description supported by theory and validated by measurements of kinetic properties, including energy distribution functions of electrons and ions. We believe that it is important to conduct such simulations and measurements with a focus on three-dimensional E×B plasma configurations with non-uniform magnetic fields, operating under the realistic plasma conditions that are encountered in plasma propulsion devices and anticipate this as a major component of any continued research project.

Our studies have taught us that the electron plasma response is crucially sensitive to the dynamics along the magnetic field direction due to high velocity of electron thermal motion. On the contrary, the motion across the magnetic field occurs on a slower time scale due to E×B drift and drifts due to magnetic field inhomogeneity and even slower drifts due to electron inertia or collisions. The ratio of the transverse to the parallel times scale can change the conditions/nature of the instabilities in a significant manner and affects anisotropy of electron velocity distribution function. Such changes can be induced by boundary conditions, by changing the geometry of the plasma set up, by driving electron fluxes along the magnetic field between electron emitting and electron absorbing walls applied to control density gradients across the magnetic field, or by shortening the plasma along the magnetic field and thereby affecting gradient-drift instabilities, or by exciting ion-acoustic instability along the magnetic field, etc.. The first approach resembles so-called segmented Hall thruster concepts proposed at PPPL more than a decade ago (Fig. 3) [6,7],

but never considered or studied in terms of its effect on plasma instabilities and plasma structures. The results of our recent study indicated that changes in boundary can strongly affect anomalous transport [8].

Accomplishments

Experiments on Penning Discharges

Experiments at PPPL were conducted primarily using the Penning discharge system (Fig. 1b). With a flexible and versatile design, this system has a convenient access for various diagnostics and can operate with well-controlled plasma parameters. In its operation, a dc voltage of 20-200 V is applied between the RF plasma cathode and the anode-chamber. The discharge can be operated with either a uniform or non-uniform magnetic field by varying the directions of the currents in the electromagnet coils or by powering coils with unequal currents. In all previous experiments, the Penning system was operated in a Helmholtz-like configuration with co-directed equal currents in both coils to produce a relatively uniform magnetic field. When operating over a relatively broad range of magnetic fields, of 30-500 Gauss, the Penning discharge sustains an efficient ionization of xenon with plasma properties (Fig. 4) [2] comparable to the plasma properties in the near anode region of the Hall thrusters where strong rotating spoke oscillations are usually observed [9].

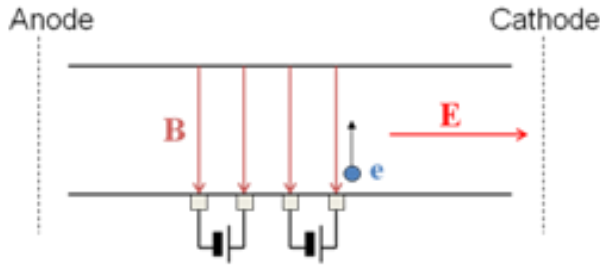

Figure 3. A PPPL concept of segmented electrode Hall thruster [7], which can be adapted for controlling of gradient driven instabilities in the proposed research.

Our measurements have revealed the presence of a spoke under almost all conditions of the magnetic field strength. These spoke oscillations are found to depend strongly on the input discharge parameters, including gas pressure and applied magnetic field (Fig. 4d). The gas type (Xe, Ar) was also shown to affect the spoke oscillation (Fig. 5). These measurements revealed that the spoke frequency follows the scaling $f \propto 1/p \times (B/m)^{1/2}$, where B is the applied magnetic field, m is the ion mass, and p is the pressure [10]. An increase in the gas pressure above 10^{-4} to 10^{-3} Torr leads to the suppression of the spoke oscillations. This scaling is different from the scaling observed in the cylindrical Hall thrusters (where $f \propto (p/B)^2 \times (1/m)^{1/2}$) [11] and magnetron discharge (where $f \propto p/B^2$ [10]). These diverse experimental scaling relationships describing the spoke dynamics in different plasma devices present a challenge to theories of rotating plasma structures. Previous studies pointed to a Modified Simon-Hoh Instability (MSHI) as one of the instabilities which could be responsible for the spoke formation in Hall thrusters. This electrostatic instability was proposed by Sakawa *et al* [12] for a Penning-type E×B system with density gradients and the electric field perpendicular to the uniform magnetic field. We showed that the MSHI occurs when $E_o/B > \Omega_{ci}L_n$, where E_o is the applied electric field, L_n is the characteristic scale of the density gradient, and Ω_{ci} is ion cyclotron frequency. According to Sakawa, the rotation frequency of MSHI-induced plasma structures is $f \propto (E/m)^{1/2}$. This theoretical result implies that the spoke should not be affected by the magnetic field or the background gas pressure if the radial electric field is constant. This contradicts our experimental findings. However, our experiments have revealed that an increase in the gas pressure decreases the value of the electric field (Fig. 4a) whereas an increase in the magnetic field leads to

an increase in the electric field. Thus, changes in these discharge parameters cause changes in the electric field. According to MHSI theory and scaling, changes in the electric field could affect this

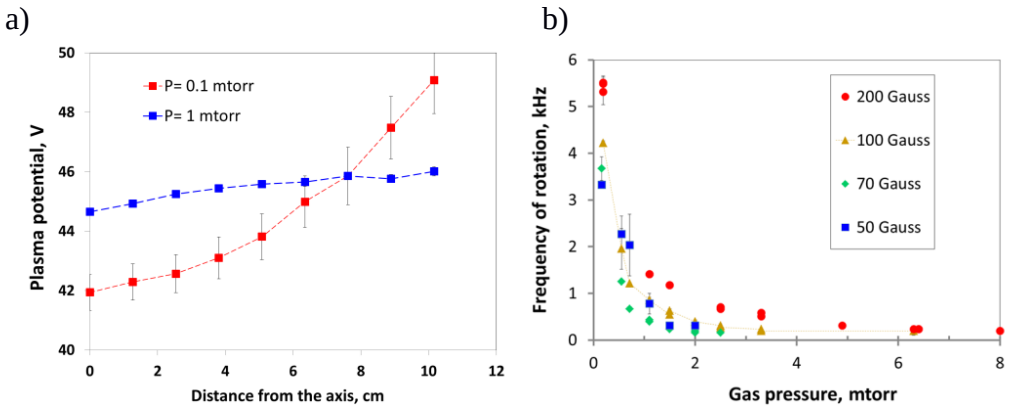

Figure 4. Gas pressure effects on the magnetized plasma in the Penning discharge. Results of electrostatic probe measurements of plasma properties across the magnetic field in the Penning discharge: plasma potential (a), rotating spoke frequency obtained from high speed imaging for different magnetic fields.

instability. The suppression of the spoke with increased pressure correlates with a strong reduction of the *E*-field (to nearly zero). Changes in the spoke frequency with *B*-field correlate with changes of *E/B* in combination.

Based on results of our PIC simulations and experimental data (discussed below), we find that to explain the spoke's behavior it is necessary to self-consistently predict the electric field as a function of discharge parameters. This is a rather complicated task because the electric field itself depends on the anomalous transport, which depends on the electric field. This makes the problem strongly nonlinear. Anomalous transport is determined not only by the spoke but also by small-scale fluctuations that may have different dependencies on the magnetic field and pressure and that may vary between E×B devices. In fact, an analysis of our experimental results using Ohm's law across the magnetic field $j = \frac{en\nu_{eff}}{m\omega_{ec}^2}\left(eE - T_e \partial n/n\partial r\right)$ suggests that the electron transport is anomalously high with ν_{eff}/ν_{col} ~ 10-100 when compared to classical collisionally-driven

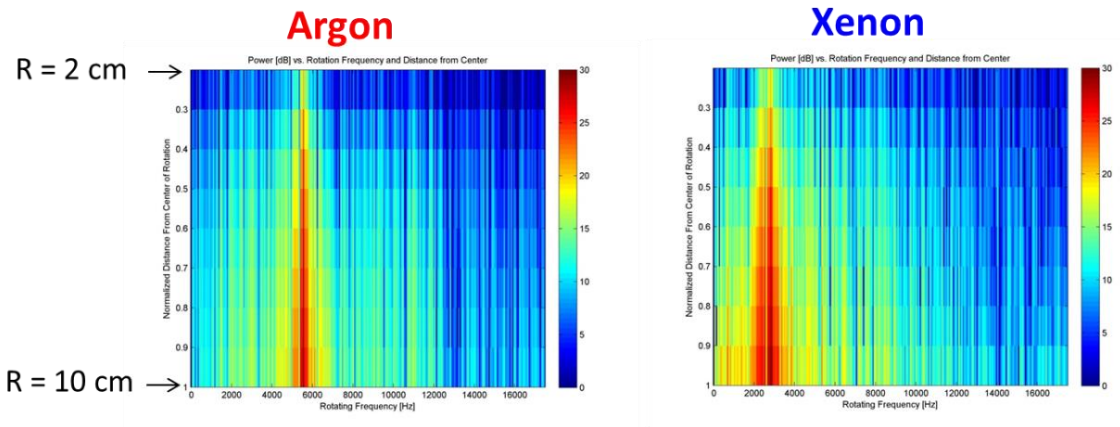

Figure 5. Local power spectrum of the normalized light intensity from fast camera images of the spoke in the Penning discharge for a given magnetic field of 50 Gauss and different gases, argon and xenon.

transport. Here, ν_{eff} is the effective electron collision frequency and ν_{col} is the collision frequency of electrons with xenon neutral atoms and ions. Remarkably, we find these results to be in fair

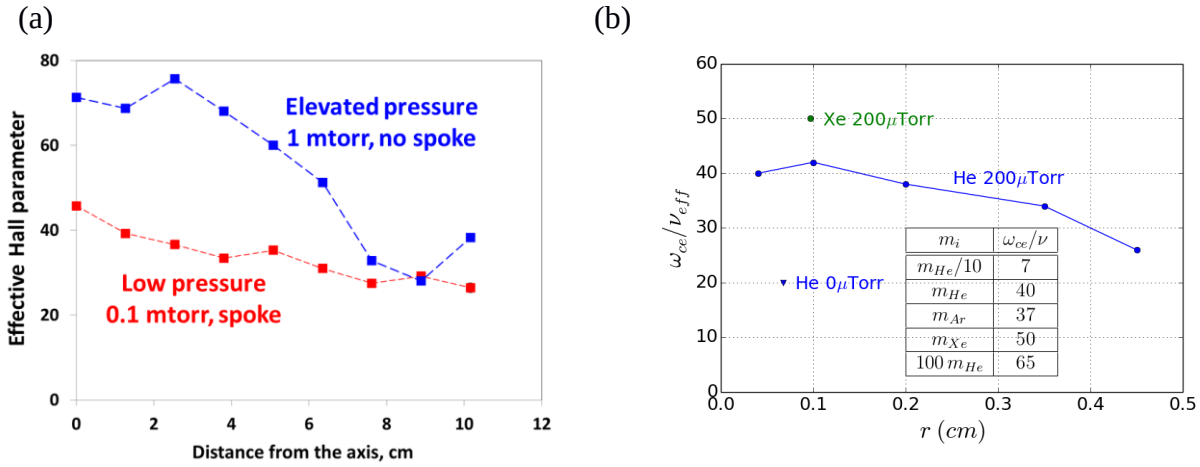

Figure 6. Effective Hall parameter ω_{ec}/ν_{eff} from (a) probe measurements and (b) PIC simulations at the B-field of 50 Gauss and two different xenon gas pressures. Table shows effect of ion mass on anomalous transport and the effective Hall parameter.

agreement with PIC simulations (Fig. 6).

Theory and Simulations Related to Penning Discharge Studies

The commercial Particle-In-Cell (PIC) code LSP has been extensively modified, benchmarked and validated for low-temperature-plasma (LTP) applications at PPPL. The standard version of LSP can perform electrostatic (ES) and electromagnetic (EM) simulations in one, two or three dimensions in Cartesian, cylindrical or spherical coordinates. It is a versatile and capable code, but has not been extensively used for LTP applications. While we perform simulations some deficiencies were found and remedied. In two- and three-dimensional simulations, we were sometimes unable to get the existing iterative ES field solver to converge the residual error to a sufficiently small value to avoid unphysical effects. We therefore took advantage of LSP flexibility to implement different ES field solver. The LSP PETSc interface was updated to support the latest version of Argonne's PETSc solver library [13]. We chose two direct ES field solvers that were implemented and have been exclusively used for our two- and three-dimensional simulations in both Cartesian and cylindrical coordinates. The direct ES solver based on the SuperLU library (called through PETSc) [**Error! Bookmark not defined.**] is very robust and memory efficient, whereas the one based on the MUMPS library is faster and more scalable [**Error! Bookmark not defined.**]. The existing external-circuit model was found to be numerically unstable due to neglecting the sheath capacitance and a new algorithm was developed and implemented. We also had to fix injection models in LSP. The model for direct injection of a particle in the simulation domain as well as model for secondary emission used fractional-weight particles. We found these models both numerically inefficient and difficult to use due to large production of particles with fractional weights. We therefore implemented injection models that create particles using a rejection method [14]. With these new injection models, all particle of a species can be guaranteed to have the same numerical weight, regardless of when and how they were created. Most of the collision models were also rewritten to use state-of-the-art algorithms, including charge exchange and anisotropy models for elastic and inelastic collisions, as well as for ionization [15]. The

modifications to the standard LSP code were deemed significant enough to justify using the name PPPL-LSP for the improved version of the code.

Benchmarking and Validation

The one-dimensional ES PIC code EDIPIC was used to benchmark LSP for a glow-discharge validation for both codes, primarily their collision models by comparison of the electric-field profile for the two codes, as well as for the experiment [16]. To get good agreement with a glow discharge, we found that a PIC code has to have very accurate collision models. A paper on this important benchmarking/validation effort is under preparation [17]. Further validation of PPPL-LSP was done for a diocotron instability frequently observed in Malmberg traps or beam experiments [18]. This proves that implemented ES solver can resolve fine structures.

Simulations of Penning discharge

Simulations were set up with PPPL-LSP code to investigate coherent structures and anomalous transport in a Penning discharge. The PIC simulations resolve thin Debye radius and fast electron plasma and cyclotron frequencies. Therefore to reduce the simulation time, the device size was reduced by and order of magnitude. We made sure that electrons are magnetized and ions are not (their corresponding gyroradius smaller and larger than discharge radius, respectively). To avoid numerical problems on the axis, Cartesian coordinates were used instead of cylindrical [19]. A homogeneous magnetic field was applied with a typical value of 100 Gauss. Similarly to experimental set up, a narrow electron beam was injected along the axis. To delineate ionization and transport mechanisms of coherent structures formations, injected beam energy was below the ionization threshold in initial simulations. The plasma was surrounded by a grounded wall (anode). For most of the simulations, the simulated device was filled with helium gas at 0.2 mTorr. In this configuration, the electric field is not externally controlled as in magnetron discharges but is established self-consistently by necessity to conduct radial current flows radially across the magnetic field, which is needed to balance the injected axial current. This configuration corresponds to experimental set up where voltage is established as a function of the cathode current, and the radial current is maintained either by an electric field or by a pressure gradient with the electron conductivity either classical or anomalous depending on plasma parameters. Therefore, the self-consistent electric field is strongly affected by density gradients and anomalous transport.

Initially, one-dimensional simulations were performed, with only the radial (x) direction numerically resolved. Without azimuthal direction being resolved, 2D modes like Simon-Hoh cannot be excited and cannot contribute to the anomalous transport [**Error! Bookmark not defined.**]. The Hall parameter values were about an order of magnitude larger than observed in the experiment. In addition to scanning the gas pressure, parameters sweeps of the ion mass and magnetic field were performed and allowed us to identify the mode responsible for the anomalous transport in the 1-D case as the lower-hybrid mode [**Error! Bookmark not defined.**].

In 2D simulations (see Fig.7), both the radial and azimuthal components are resolved, which allows many more modes to get excited and contribute to the anomalous transport. Even with the reduced device size, the two-dimensional simulations are somewhat large. 500 x 500 cells are used to resolve the Debye sphere in the plane orthogonal to the axial magnetic field and the injected electron beam, and a time step of 5ps is used to resolve the plasma oscillation. 25 macro particles of each species per cell were found to be sufficient (quadrupling the number did not significantly change the result). With these parameters, simulating 5us (one million time steps) takes just over three days on 256 processor cores on a cluster with Intel Xeon processors connected with

InfiniBand. To date, Penning-discharge simulations have been performed using over 370,000 core-hours, equivalent to two months of run time on 256 cores. The primary parameters scanned have been the ion mass, gas pressure and magnetic field [**Error! Bookmark not defined.**]. The physics is more complicated in two dimensions and will require more analysis, but the mass and pressure scaling of the Hall parameter seem to be in good agreement with experiment as shown in Fig. 6.

The spoke dynamics is complicated and it is difficult to determine a single spoke frequency. The frequency spectrum is very broad and has a radial dependence. The two-dimensional simulations exhibit rich physics that need more theoretical analysis. Excitation of anti-drift and low hybrid modes together makes analysis complex

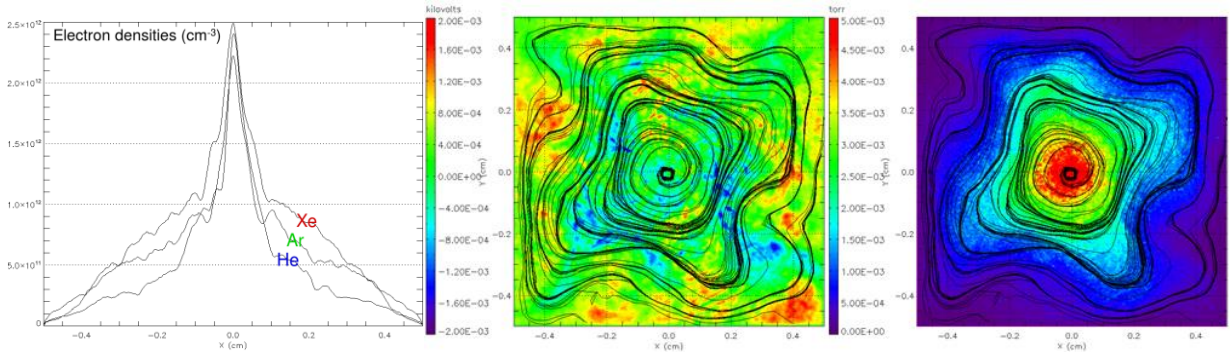

Figure 7. Density profile (left) is peaked in the center and is different for different ion masses (He, Ar, Xe), similarly to experimentally observed. Current streamlines on top of potential contours (middle) and electron-pressure contours (right) at 2 μs.

Experiments on Small Low Power Magnetron Discharges

The magnetron discharge studied at Stanford is shown schematically in Fig. 8. Shown in the figure is the configuration that generates a 5 mm diameter toroidal discharge described in several publications [20 – 23]. As part of this program, we have also constructed a 19 mm diameter plasma of a similar construction [24] (see photo in Fig. 9). In this configuration, the plasma forms between a graphite cathode and a transparent indium tin oxide anode providing direct optical access for emission and laser-induced fluorescence studies. In the 5 mm diameter discharge variant, a 17 mm diameter Co-Sm ring magnet with an iron core generates the magnetic field topology. The maximum field at the cathode is ~1 T. Axial gradients are generated in both the plasma density and magnetic field. These gradients drive rotating structures that are attributed to resistive drift instabilities (see theory below). The frequency that we see in these discharges is much higher than the rotating structures seen in the Penning discharges and the mode structures depend on operating conditions.

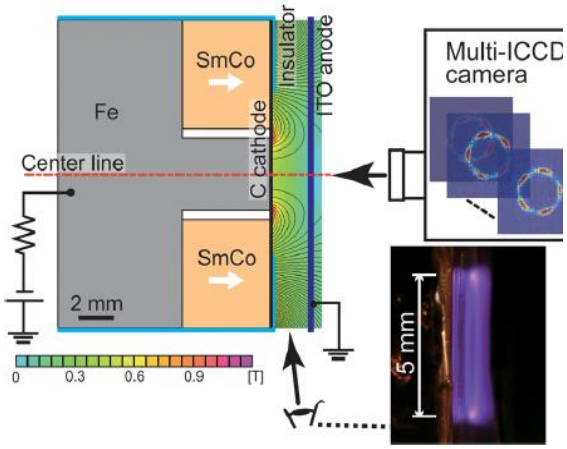

Figure 8. Schematic of 5 mm diameter magnetron discharge plasma. Insets show high speed camera frames of emission recorded through the ITO anode, and side photos taken with a standard DSLR camera.

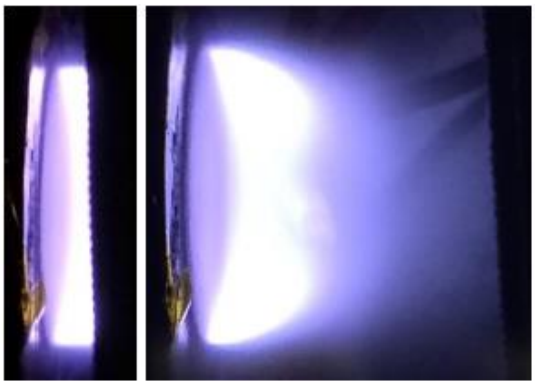

Figure 9. DSLR side-view photograph of the 19 mm diameter discharge. The left is the case of a relatively small (~4 mm gap), whereas the right is a > 20 mm gap. The discharge shown here is operating on xenon.

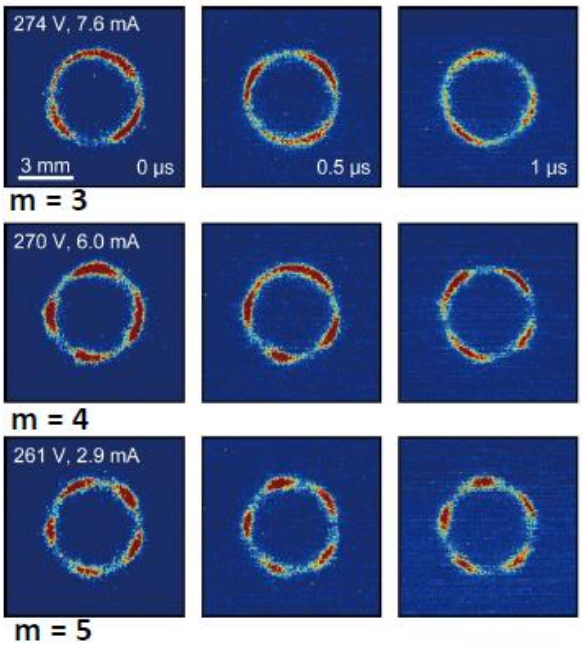

Figure 10. Frames from a high speed camera of emission through the ITO anode depicting rotating structures and their mode-dependence on discharge voltage.

We have developed a theory for the rotating structures, with the goal of predicting the frequency dependence with discharge voltage (E-field) and the mode transitions seen with varying discharge voltage. As described below the theory treats the disturbances as drift waves driven by axial gradients in both density and magnetic field. The structures are well defined and very coherent (see Fig. 10), rotating at speeds of $2 – 4 \times 10^3$ m/s – considerably lower than the local drift velocity (~5×10^4 m/s). The direction of these coherent modes all seem to be in the – E x B direction. We note however that the direction of the external field may not necessarily be the direction of the local field, as we discuss below.

The mode structure seems to be very sensitive to variations in the discharge voltage, undergoing very abrupt transitions. Within a particular mode, the mode frequency appears to be inversely dependent on discharge voltage (see Fig. 11, left frame). Increasing discharge voltage results in transitions toward higher mode number (shorter wavelength) as can be seen in Figs. 10 and 11. Our theoretical studies suggest that the mode transitions are due to the strong wavelength-dependence of the cut-off in the growth rate of this gradient drift instability. Analysis carried out with segmented ITO anodes confirm the rotational structure seen in the high speed video (see Fig. 11, right frame). A wavelet dispersion analysis confirms this strong coherence, with a resonant frequency at 250 kHz and a wavenumber ($1/\lambda$) of 200 m^{-1}. A spectral power density verses frequency extracted from any of the anode segments shows activity between 10 and 50 MHz. A bi-coherence analysis suggests the possibility of wave-wave interactions between 15 and 30 kHz [24]. It is noteworthy that although the current in each segment fluctuates strongly, as shown in the right frame of Fig. 11, the sum of the currents through the three segments as well as the remaining anode segment (see inset in Fig. 11-right) results in a nearly non-fluctuating total current. This implies that these structures conduct the entire discharge current. The discharge current is anomalous (i.e., cannot be accounted for by classical scattering collisions) and so, as was found in the studies of the Penning discharge, implies that these structures are responsible for driving anomalous cross field transport. The predicted

frequencies are in good agreement with experimental trends (Fig. 11). The theory (discussed

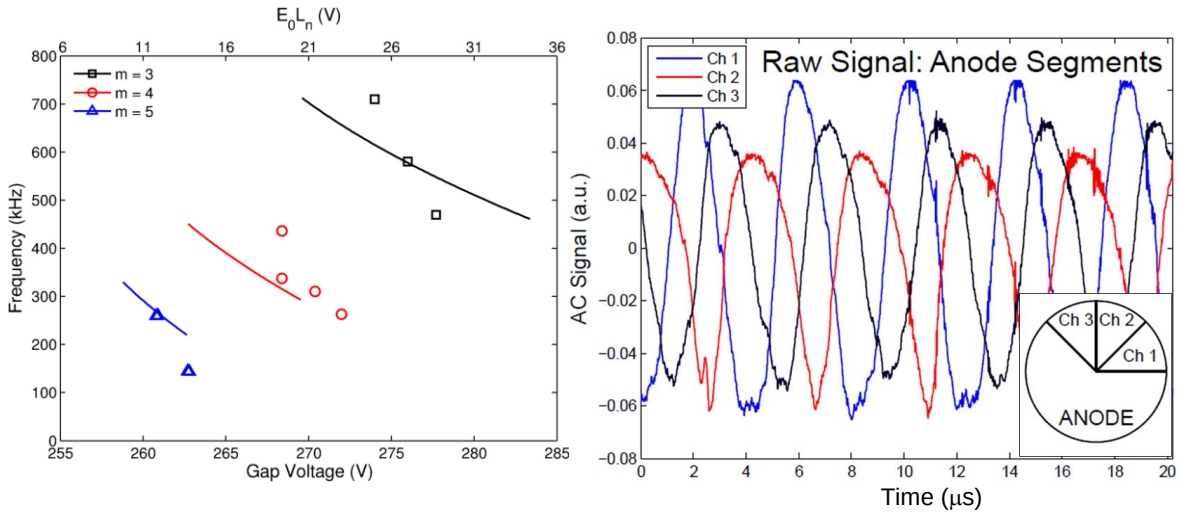

Figure 11. (left) Measured and predicted rotation frequency vs. voltage. (right) Segmented anode signals during a strong m = 3 azimuthal mode.

below) predicts the frequencies to scale as $f \propto (E_o / m)^{1/2}$, similar to that suggested by the studies of Sakawa et al [12].

Interesting features are observed when the voltage is set such that the system resides in a metastable state between modes m = 3 and m = 4, or between m = 4 and m = 5. In these metastable states, the signal in any single anode segment fluctuates in a somewhat random manner, as depicted in the left frame of Fig. 12. The fluctuation seems to be quasi-turbulent. High speed images reveal considerable absence of coherence, and the segmented anode, which serves also as a probe of the local current fluctuation, show a rich blend of frequencies, with fluctuations at very high frequencies, well above the frequency of the coherent state. The panel on the right side of Fig. 12 shows a spectral power distribution. Note strong frequencies as high as 3.5 MHz, with nearly all

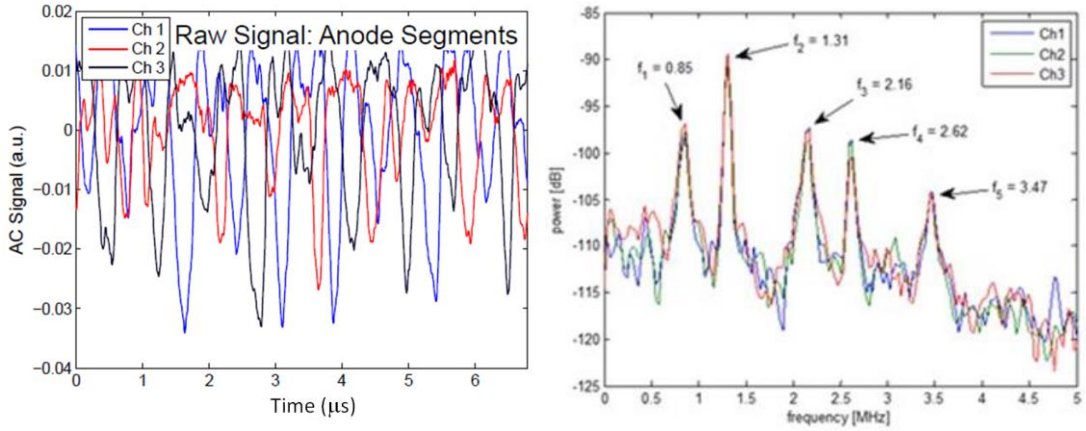

Figure 12. (left) Segmented anode signals when state is between m = 4 and m = 5. (right) Corresponding power spectral plot with five dominant frequencies indicated.

of the frequencies higher than the frequencies of the coherent modes for the adjacent m = 4 or m = 5 disturbances. The higher frequencies suggest a non-linear mechanism for energy redistribution.

A simple assignment of the main frequency components suggests a non-linear wave-wave interaction typical of a turbulent energy cascade. For example, for the results shown, we see that there are five dominant frequencies associated with this "turbulence". We see by inspection that to a great extent, $f_1+f_2 = f_3$, and $f_2+f_3 = f_5$, suggesting several three-wave coupling possibilities. The wave dispersion map (see Fig. 13) from the current that is collected by the three segments also suggest that the wavenumbers of these interactions confirm a possible three wave coupling, although the size of the segments (as seen from the inset of the left frame in Fig. 11) preclude this assignment with certainty. We also investigated the characteristics of the discharge over higher frequency ranges (up to 250 MHz) and found between 10-40 MHz a fast mode propagating in the negative E×B direction with a phase velocity of ~2×10^6 m/s. A wavelet analysis indicated the existence of high turbulence intensities near the main wave propagation modes indicative of energy dissipation at these frequencies. This fast wave seems to propagate independently of the lower frequency modes, whether these modes are well organized or not.

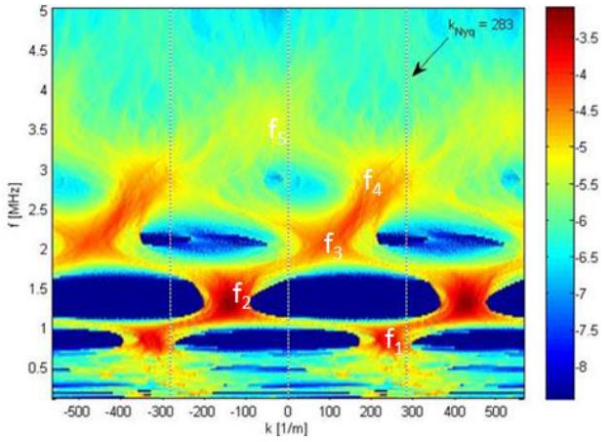

Figure 13. Wave dispersion map associated with the fluctuations captured by segmented anode when the discharge state is between coherent modes m = 4 and m = 5.

Theory of Drift Waves in Small Low Power Magnetron Discharges

Because of the relatively high pressure (~10–20 Pa) and plasma densities (~10^{13} cm^{-3}), the plasma in these magnetron discharges is quasi-neutral. The millimeter scale produces strong plasma and magnetic field gradients (~10^{14} cm^{-4} and 5 T/cm, respectively), and, as a consequence, we interpret our results using models for gradient-driven drift instabilities originally developed to explain low frequency waves seen in Hall thrusters [25, 26]. We extend the model of Ref. 26 to include transport along the magnetic field, expanding the domain of instability. The model results are in good agreement with the observed experimental behavior: waves propagate in the −E ×B direction with frequencies between 100 and 500 kHz exhibiting strong dependency on the local electric field. To obtain this agreement, we must assume a field reversal within the discharge, which is plausible when density gradients are strong and diffusion drives more anode-bound electrons than demanded by the external circuit. Field reversals are commonly seen in hybrid simulations of Hall thrusters (in the anode region), and one was recently hypothesized to explain electron heating and unsteady behavior [27] and enhanced ion back-flow [28] in HiPIMS sources.

The analysis considers a two-dimensional, two-fluid model where the ions are non-magnetized and electrons are strongly magnetized. We unfold the annular geometry onto a Cartesian coordinate system with an electric field E_o oriented along the discharge axis ($\hat{x}$-direction, positive from anode to cathode), and a magnetic field B_o taken primarily along the $\hat{z}$-direction (radially outwards). The background plasma (assumed uniform in the $\hat{y}$-direction) contains plasma density (n_o) and magnetic field gradients along the $\hat{x}$-direction, as illustrated qualitatively in Fig. 14. We

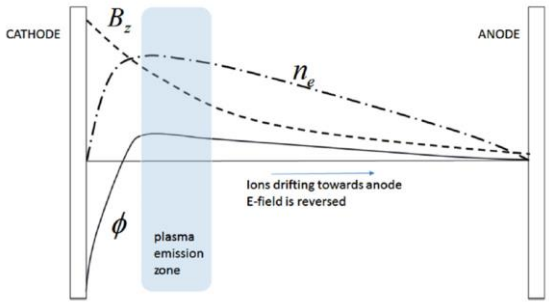

Figure 14. Illustration of the assumed plasma structure within the discharge for the gradient-drift model.

presume that the strongest ionization and emission occur just beyond the cathode fall, where plasma density gradients near the anode produce a field reversal, $E_o < 0$, driving ions towards the anode. An analogous reverse ion migration was measured by laser induced fluorescence in the near anode region of Hall thrusters [29], highlighting one of the possible the similarities between these DC magnetrons and Hall discharge thrusters.

Linearized species continuity and momentum equations for the plasma constituent number densities and velocities are subject to Fourier perturbations to describe the dispersion conditions for wave propagation. The quiescent plasma electrons experience diamagnetic (isothermal) and $E \times B$ drifts, respectively, that lead to the following equation for the plasma density [30]:

$$\frac{\partial n_e}{\partial t} + \vec{v}_{eD} \cdot \nabla n_e - 2n_e\left(\vec{v}_{eD} + \vec{v}_{eE\times B}\right)\cdot \nabla \ln \vec{B}_o + \frac{\partial n_e v_{ez}}{\partial t} = 0$$

This equation differs from that in Ref. 26 by the last term, which describes diffusion along the magnetic field lines. As in Ref. 30, we assume electron/ion collisionality along the B-parallel ($\hat{z}$-direction) only. Invoking quasi-neutrality, the electrons and ions diffuse together with a $\hat{z}$-directed flux, $\Gamma_{e,i_z} = -D_A \partial n_e \partial z$. Here, D_A is the ambipolar diffusion coefficient.

By carrying out the usual perturbation analysis and linearizing the equations, we find the following dispersion relation for the frequency (ω) dependence on wavenumber components perpendicular to B_o ($k_\perp$) and parallel to E_o (k_x):

$$\omega^2 - \left(2k_x v_{io} + \frac{k_\perp^2 c_s^2}{\omega^* - \omega_D}\right)\omega + k_x^2 v_{io}^2 + \frac{k_\perp^2 c_s^2\left(\omega_o + \omega_D\right)}{\omega^* - \omega_D} - i\frac{k_\perp^2 c_s^2 \nu_c}{\omega^* - \omega_D} = 0$$

Here, $c_s = (kT_e/m_i)^{1/2}$ is the ion acoustic speed, v_{io} is the ion drift velocity due to the external electric field, $\nu_c = k_z^2 D_A$ is the collisional dissipation rate, $\omega^* = k_y v_{eD}$, $\omega_o = k_y v_{eE\times B}$ and $\omega_D = -2kT_e / eB_o L_B$. In the absence of the diffusive term, the dispersion will have identical characteristics to that derived in Ref. 26, and, with E_o (and v_{io}) < 0, the region of instability has a distinct long wavelength cutoff that depends on background plasma conditions. We calculate the predicted growth rate of the unstable branch (imaginary component of the dispersion solution assuming real wavenumbers) using experimental conditions, E_o=−11.6 kV/m, L_n=2 mm ($E_o L_n$=−23.1 V), L_B=0.5 mm, kT_e =3.1 eV, B_o=0.6 T, k_x =7.0 mm^{-1}, k_z=2.5 mm^{-1}, and v_{io} = –933 m/s, and plot the result as the solid line in Fig. 15(top). The maximum growth rate is somewhere between m = 3 and m = 4, and increasing the electric field shifts the cutoff and peak towards longer wavelengths. Including the diffusive term (using $\nu_i = 5 \times 10^7$ s^{-1}) modifies the growth rate, extending the region of instability

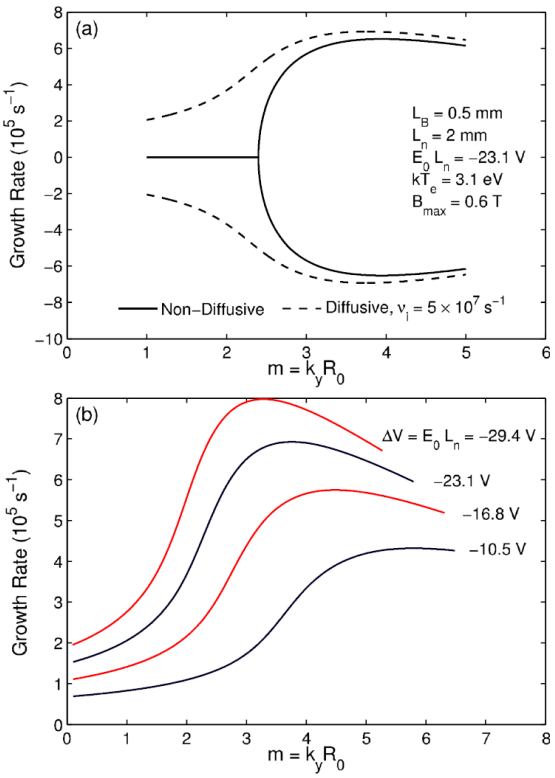

Figure 15. (a) Growth rate of the instability versus mode number for the diffusive (dashed) and non-diffusive (solid) cases. (b) Growth rate variation with mode number computed for a range of values of the voltage "hump".

beyond the original cutoff (see the dotted line in Fig. 15(a)). As the discharge voltage increases, we expect an active m = 4 mode until the peak growth rate passes a critical value, triggering a mode transition to m = 3. The variation in the peak growth rate with electric field is shown in Fig. 15(b). When increasing the field, we assume a simple scaling that $kT_e \sim E_o$ and $\nu_{io} \sim E_o^{1/2}$.

The real component of the frequencies of the unstable root tends to decrease with increased electric field while within the range of instability for any single mode. As illustrated by the solid lines in Fig. 11 (left frame), once a new mode is preferred (higher m for voltage increases), a jump in frequency is predicted. To compare the experiments with the model, we have assumed that a 12 V voltage "hump" ($E_o L_n$) is generated when the discharge voltage is 261 V. No other adjustments are made to the predicted dispersion. The values chosen for various plasma parameters are the same as those listed above and used in Fig. 15. Agreement with experiments is good, considering the uncertainties in the properties used as base conditions. A model tested without including the diffusive terms fails to achieve such an agreement.

The low power DC magnetron studied as part of this project is an excellent test bed for understanding ordered (coherent) structures, which we believe can be attributed to gradient-driven instabilities in cross-field discharges. The observed mode transitions are distinct, coherent, and reproducible. A simple theory for the dispersion of these gradient-driven drift waves seems to describe these instabilities quite well. The success of the model rests heavily on the presumption of a field reversal, generating a voltage "hump" that drives a reverse (anode-directed) ion flow, and future experiments will seek confirmation of such a structure. Our anticipation is that advanced diagnostics will enable validating this field reversal, and hence the essential physics needed to drive the rotation of these structures in a direction opposite to the imposed electric field.

One note in point is that the frequencies of these structures are nearly ~1MHz. We believe that these structures can be driven to higher frequencies with external forcing. Their external control can enable new applications such as in the control of electromagnetic waves in photonic crystal waveguide filters.

Publications from this Research

1. Carlsson, Johan A., Igor D. Kaganovich, Alexander V. Khrabrov, Andrei Smolyakov, Dmytro Sydorenko, and Yevgeny Raitses. "Multi-dimensional kinetic simulations of instabilities and transport in EXB devices." In Plasma Sciences (ICOPS), 2015 IEEE International Conference on, pp. 1-1. IEEE, 2015.
2. Smolyakov, A., I. Romadanov, W. Frias, J. Carlsson, I. Kaganovich, and Y. Raitses. "Small scale instabilities and anomalous electron current in Hall plasmas." Bulletin of the American Physical Society 60 (2015).
3. Smolyakov, A., I. Romadanov, W. Frias, A. Koshkarov, A. Y. Raitses, and I. Kaganovich. "Instabilities and transport in plasmas with EXB drift." In Plasma Sciences (ICOPS), 2015 IEEE International Conference on, pp. 1-1. IEEE, 2015.
4. Carlsson, Johan, Igor Kaganovich, Alexander Khrabrov, Yevgeny Raitses, and Andrei Smolyakov. "Two-and three-dimensional particle-in-cell simulations of ExB discharges." Bulletin of the American Physical Society 60 (2015).
5. Smolyakov, A., W. Frias, I. Romadanov, I. Kaganovich, Y. Raitses, and M. Umansky. "Anomalous electron transport in magnetized plasmas with ExB drift." Bulletin of the American Physical Society 60 (2015).
6. Ito, Tsuyohito, Christopher V. Young, and Mark A. Cappelli. "Self-organization in planar magnetron microdischarge plasmas." Applied Physics Letters 106, no. 25 (2015): 254104.
7. Young, Chris, Nicolas Gascon, Andrea Lucca Fabris, Mark Cappelli, and Tsuyohito Ito. "Laser induced fluorescence measurements of ion velocity in a DC magnetron microdischarge with self-organized drift wave modes propagating in the direction opposite the E x B electron drift velocity." Bulletin of the American Physical Society 60 (2015).
8. Young, Christopher, Nicolas Gascon, Andrea Lucca Fabris, Tsuyohito Ito, and Mark Cappelli. "Ion dynamics in a DC magnetron microdischarge measured with laser-induced fluorescence." Bulletin of the American Physical Society 60 (2015).
9. Fabris, A. Lucca, C. V. Young, and M. A. Cappelli. "Excited state population dynamics of a xenon ac discharge." Plasma Sources Science and Technology 24, no. 5 (2015): 055013.
10. Frias, Winston, Andrei I. Smolyakov, Igor D. Kaganovich, and Yevgeny Raitses. "Wall current closure effects on plasma and sheath fluctuations in Hall thrusters." Physics of Plasmas (1994-present) 21, no. 6 (2014): 062113.
11. Y. Raitses, I. D. Kaganovich and A. Smolyakov, Effects of the Gas Pressure on Low Frequency Oscillations in E X B Discharges, IEPC-2015-307 /ISTS-2015-b-307, Joint Conference of 30th International Symposium on Space Technology and Science 34th International Electric Propulsion Conference and 6th Nano-satellite Symposium, Hyogo-Kobe, Japan July 4-10, 2015.
12. J. Carlson, I. Kaganovich, A. Khrabrov, Y. Raitses, A. Smolyakov, and D. Sydorenko, “Multi-Dimensional Kinetic Simulations of Instabilities and Transport in ExB Devices”, IEPC-pare 2015-373, the 34th International Electric Propulsion Conference, Hyogo-Kobe, Japan, July 4 – 10, 2015.
13. W. Frias, Pombo , A. I. Smolyakov, I. Romadanov, Y. Raitses, I. D. Kaganovich, and M Umansky, "Small scale fluctuations and anomalous electron current in Hall plasmas" IEPC-2015-370／ISTS-2015-b-370, the 34th International Electric Propulsion Conference, Hyogo-Kobe, Japan, July 4 – 10, 2015.
14. Y. Raitses, A. Smolyakov , I. D. Kaganovich, "Coherent Plasma Structures in Crossed-Field Discharge Devices", I2.J101, Proceedings of the 42nd EPS Conference on Plasma

Physics

15. B. Kraus and Y. Raitses, " Probe Techniques for Plasma Potential Measurements in a Low-Temperature Magnetized Plasma" JP12.164, Bulletin of American Physical Society,.Division of Plasma Physics, 2015.

References

[1] Y. Raitses, A. Smirnov, and N. J. Fisch, Phys. Plasmas 16, 057106 (2009).
[2] Y. Raitses, JANNAF paper 3984, 2015
[3] J. B. Parker, Y. Raitses, and N. J. Fisch, Appl. Phys. Lett. **97**, 091501 (2010)
[4] M. McDonald and A. D. Gallimore, IEEE Trans. Plasma Sci. **11** 2952 (2011).
[5] W. Frias, A. I. Smolyakov, I. D. Kaganovich, and Y. Raitses, Phys. Plasmas **19**, 072112 (2012).
[6] N. J. Fisch, Y. Raitses, A. Litvak, L. A. Dorf, AIAA paper- 99-2572, Los Angeles, CA, 1999.
[7] Y. Raitses, M. Keidar, D. Staack and N. J. Fisch, J. Appl. Phys. **92**, 4906 (2002).
[8] A. I. Smolyakov, W. Frias, I. Kaganovich, Y. Raitses, Phys. Rev. Lett. **111**, 115002 (2013).
[9] C. L. Ellison, Y. Raitses and N. J. Fisch, Phys. Plasmas **19**, 013503 (2012).
[10] Y. Raitses, A. Smolyakov, I. D. Kaganovich, IEPC paper 2015-307, Kobe, Japan, 2015.
[11] Y. Raitses, J. B. Parker, E. Davis, and N. J. Fisch, AIAA 2010 paper -6775 (2010).
[12] Y. Sakawa, C. Joshi, P. K. Kaw, F. F. Chen, and V. K. Jain, Phys. Fluids B **5**, 1681 (1993).
[13] Argonne's PETSc solver library http://www.mcs.anl.gov/petsc/ .
[14] N. Radford, Annals of Statistics **31** (3): 705–767 (2003).
[15] A. V. Khrabrov, and I. D. Kaganovich, Phys. Plasmas **19**, 093511 (2012); A. Okhrimovskyy, A. Bogaerts, and R. Gijbels, Physical Review E **65**, 037402 (2002).
[16] Den Hartog, E. A., D. A. Doughty, and J. E. Lawler, Physical Review A **38**, 2471 (1988).
[17] J. A. Carlsson, I. D. Kaganovich, A. V. Khrabrov, Y. Raitses, A. Smolyakov, D. Sydorenko, IEPC/ISTS paper 2015-373, Kobe, Japan, 2015
[18] G. Rosenthal, G. Dimonte, and A. Y. Wong, Physics of Fluids **30**, 3257 (1987)
[19] K. Matyash, R. Schneider, Y. Raitses, N. J. Fisch, in Proc. IEPC-2011- 070 paper , 2011.
[20] T. Ito and M. A. Cappelli, IEEE Trans. Plasma Sci. 36, 1228 (2008).
[21] T. Ito and M. A. Cappelli, Appl. Phys. Lett. 94, 211501 (2009).
[22] T. Ito and M. A. Cappelli, Appl. Phys. Lett. 89, 061501 (2006).
[23] T. Ito, N. Gascon, W. S. Crawford, and M. A. Cappelli, J. Propul. Power 23, 1068 (2007).
[24] C. Young, N. Gascon, A. Lucca Fabris, M. Cappelli, and T. Ito. Bulletin of the American Physical Society 60 (2015).

[25] A. Kapulkin and M. M. Guelman, IEEE Trans. Plasma Sci. 36, 2082 (2008).
[26] W. Frias, A. I. Smolyakov, I. D. Kaganovich, and Y. Raitses, Phys. Plasmas 19, 072112 (2012).
[27] A. Anders, Appl. Phys. Lett. 105, 244104 (2014).
[28] N. Brenning, C. Huo, D. Lundin, M. A. Raadu, C. Vitelaru, G. Stancu, T. Minea, and U. Helmersson, Plasma Sources Sci. Technol. 21, 025005 (2012).
[29] N. B. Meezan, W. A. Hargus, Jr., and M. A. Cappelli, Phys. Rev. E 63, 026410 (2001).
[30] J. C. Perez, W. Horton, K. Gentle, W. Rowan, K. Lee, and R. B. Dahlburg,
Phys. Plasmas 13, 032101 (2006).

1.

1. Report Type

Final Report

Primary Contact E-mail

Contact email if there is a problem with the report.

cap@stanford.edu

Primary Contact Phone Number

Contact phone number if there is a problem with the report

650-723-1745

Organization / Institution name

Stanford University

Grant/Contract Title

The full title of the funded effort.

Coherent Structures in Plasma Relevant to Electric Propulsion

Grant/Contract Number

AFOSR assigned control number. It must begin with "FA9550" or "F49620" or "FA2386".

FA9550-14-1-0017

Principal Investigator Name

The full name of the principal investigator on the grant or contract.

Mark Cappelli

Program Manager

The AFOSR Program Manager currently assigned to the award

Mitat Birkan

Reporting Period Start Date

05/15/2014

Reporting Period End Date

03/14/2016

Abstract

Magnetized plasmas in E x B configurations exhibit complex behavior resulting in variety of turbulent and coherent fluctuations that can critically affect E x B plasma thruster devices and performance. Rotating structures have been observed in laboratory and technological plasma devices with magnetized electrons and non-magnetized ions. These oscillations have low mode number with a characteristic frequency that lies between the electron and ion gyro-frequencies. Experimental studies of Hall and Penning discharges demonstrated that low frequency (10's kHz) disturbances contribute to electron cross-field transport. Studies carried out in mesoscale magnetrons place these coherent fluctuations at much higher frequencies (100's of kHz) and also contribute substantially to the electron transport. For Hall thrusters, electron cross-field transport is of practical importance because it diminishes the thrust efficiency. Fluctuation-induced transport reduces the local electric field, potentially leading to increased plume divergence and thruster wall erosion. This program is to better understand the physics behind these fluctuations and their relevance to propulsion devices through experimental, theoretical, and numerical studies.

Distribution Statement

This is block 12 on the SF298 form.

Distribution A - Approved for Public Release

Explanation for Distribution Statement

If this is not approved for public release, please provide a short explanation. E.g., contains proprietary information.

SF298 Form

Please attach your SF298 form. A blank SF298 can be found here. Please do not password protect or secure the PDF
The maximum file size for an SF298 is 50MB.

Form SF298_AFD-070820-035.pdf

Upload the Report Document. File must be a PDF. Please do not password protect or secure the PDF . The maximum file size for the Report Document is 50MB.

AFOSR Final Technical Report Stanford-Princeton.pdf

Upload a Report Document, if any. The maximum file size for the Report Document is 50MB.

Archival Publications (published) during reporting period:

2. New discoveries, inventions, or patent disclosures:
Do you have any discoveries, inventions, or patent disclosures to report for this period?

No

Please describe and include any notable dates

Do you plan to pursue a claim for personal or organizational intellectual property?

Changes in research objectives (if any):

Change in AFOSR Program Manager, if any:

Extensions granted or milestones slipped, if any:

AFOSR LRIR Number

LRIR Title

Reporting Period

Laboratory Task Manager

Program Officer

Research Objectives

Technical Summary

Funding Summary by Cost Category (by FY, $K)

	Starting FY	FY+1	FY+2
Salary			
Equipment/Facilities			
Supplies			
Total			

Report Document

Report Document - Text Analysis

Report Document - Text Analysis

Appendix Documents

2. Thank You

E-mail user

Jun 17, 2016 18:17:58 Success: Email Sent to: cap@stanford.edu